Journal of Sound and Vibration (2001) **245**(4), 653–667
doi:10.1006/jsvi.2000.3557, available online at http://www.idealibrary.com on IDEAL®

FREE VIBRATION OF A LAMINATED CIRCULAR RING SEGMENT

B. KOVÁCS

Institute of Mathematics, University of Miskolc, Miskolc-Egyetemváros, Hungary 3515.
E-mail: matmn@uni-miskolc.hu

(*Received* 18 *April* 2000, *and in final form* 15 *December* 2000)

A new laminate model is presented for the dynamic analysis of a laminated circular ring segment. The differential equations which govern the free vibrations of a circular ring segment and the associated boundary conditions are derived by Hamilton's principle considering bending and shear deformation of all layers. The author used a new iterative process to successively refine the stress/strain field in the viscoelastic layer. The model includes the effects of transverse shear and rotatory inertia. The iterative model is used to predict the modal frequencies and damping of a simply supported sandwich circular arch. The solutions for a three-layer circular arch are compared to a three-layer approximate model.

1. INTRODUCTION

Laminated composite curved beams have been used in engineering applications for many years. Design applications of isotropic and curved bars, rings and arches of arbitrary shapes are assisted by a well-developed theory and proven design guidelines [1–4]. The development of the theory and design guidelines for composite curved beams is much less satisfactory. Earlier works are related to the sandwich beams or closed composite rings [5–9]. The finite element method was used to study the dynamic response of sandwich curved beams by Ahmed [5, 6]. Free and forced vibrations of a three-layer damped ring were investigated by Di Taranto [7]. Lu and Douglas [8] investigated a damped three-layered sandwich ring subjected to a time harmonic radially concentrated load. Their paper gives an analytical solution for the mechanical impedance at an arbitrary point on the surface of the damped structure as a function of the forcing frequency. Furthermore, an experimental procedure is employed to measure the driving point mechanical impedance as a verification of the calculated results. The transient response was studied for three-layer closed rings by Sagartz [9]. The damping properties of curved sandwich beams with a viscoelastic layer were studied by Tatemichi *et al.* [10]. Viscoelastic damping in the middle core layer was emphasized.

Nelson and Sullivan [11] analyzed a complete circular ring consisting of a layer of soft viscoelastic material sandwiched between two hard elastic layers. The equations which govern the forced vibration of a damped circular ring were solved by the method of damped forced modes. Isvan and Nelson [12] investigated the natural frequencies and composite loss factors of the free vibration of a soft cored circular arch simply supported at each end. Kovacs [13] solved the problem of free vibrations of a stiff-cored sandwich circular arch. All

0022-460X/01/340653 + 15 $35.00/0

the tangential displacement components are assumed to be piecewise linear across the thickness, thus implying the inclusion of shear deformations and rotary inertia.

The incremental equations of motion based on the principle of virtual displacements of a continuous medium are formulated using the total Lagrangson description by Liao and Reddy [14]. They developed a degenerate shell element with a degenerate curved beam element as a stiffener for the geometric non-linear analysis of laminated, anisotropic, stiffened shells. Bhimaraddi *et al.* [15] presented a 24 d.o.f. of an isoparametric finite element for the analysis of generally laminated curved beams. The rotary inertia and shear deformation effects were considered in this study. Qatu developed a consistent set of equations for laminated shallow and deep arches [16, 17] . Exact solutions are presented for laminated arches having general boundary conditions by Qatu and Elsharkawy [18]. The in-plane free vibrational analysis of symmetric cross-ply laminated circular arches is studied by Yildirim [19]. The free vibration equations are based on the distributed parameter model. The transfer matrix method is used in the analysis. The rotary inertia, axial and shear deformation effects are considered in the Timoshenko analysis by the first order shear deformation theory. Vaswani *et al.* [20] derived a closed-form solution for the system loss factors and resonance frequencies for a curved sandwich beam with a viscoelastic core by the Ritz method. He and Rao [21] used the energy method and Hamilton's principle to derive the governing equation of motion for the coupled flexural and longitudinal vibration of a curved sandwich beam system. Both shear and thickness deformations of the adhesive core are included. Equations for obtaining the system modal loss factors and resonance frequencies are derived for a system having simply supported ends by the Ritz method.

It is well known that the accurate determination of the stress field in the laminate configurations is particularly important for "stress-critical" calculations such as damping and delamination. Zapfe and Lesieutre [22] developed an iterative process to refine successively the shape of the stress/strain distribution for the dynamic analysis of laminated beams. The iterative model is used to predict the modal frequencies and damping of simply supported beams with integral viscoelastic layers.

The present research extends the iterative laminated model developed by Zapfe and Lesieutre to the dynamic analysis of a laminated circular ring segment. The current model is developed for the specific case of a simply supported circular ring segment with uniform properties along its length.

2. GOVERNING EQUATIONS OF MOTION

The geometry of interest and the notation used are shown in Figure 1. As indicated in the figure, the ring segment ends are simply supported. Consider the curved sandwich arch with a circular centreline and a constant rectangular cross-section. The arch consists of three different layers of homogeneous materials bonded together to form a composite arch. Subscript i, where $i = 1$–3 is used to denote quantities in the various layers, starting from the outermost layer, so that layers 1 and 3 represent the elastic layers while 2 represents the viscoelastic layer. A state of plane stress is assumed, as well as the fact that the materials in each layer of the arch are homogeneous isotropic. A perfect bonding of the layers and linear elasticity are also assumed in the analysis. The composite arch is lightly damped and it is assumed that all the energy dissipated is dissipated in the viscoelastic layer. The deformation in the radial direction is neglected. An initial cross-section of the first layer such as A_1A_2 deforms to $A'_1A'_2$ as shown in Figure 2. This simply means that the plane cross-sections in the individual layer continue to remain plane after deformation. Keeping in mind that the deformation in the radial direction is neglected, such continuous

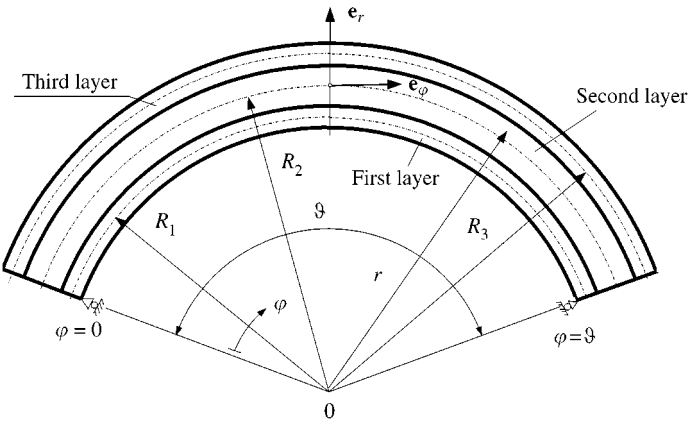

Figure 1. The geometry of the laminated circular ring segment.

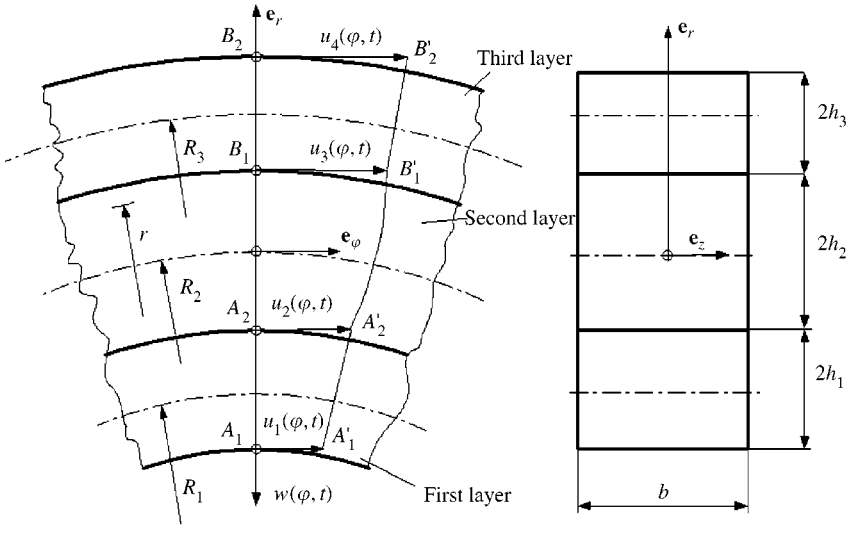

Figure 2. The displacement field of the laminated circular ring segment.

displacements of cross-sections are described by the following displacement field:

$$\mathbf{t}_1(r, \varphi, t) = \frac{1}{2h_1}[(h_1 + r - R_1)u_2(\varphi, t) + (h_1 - r + R_1)u_1(\varphi, t)]\mathbf{e}_\varphi - w(\varphi, t)\mathbf{e}_r,$$

$$R_1 - h_1 \leqslant r \leqslant R_1 + h_1. \tag{1}$$

In the above equation $u_1(\varphi, t)$ and $u_2(\varphi, t)$ denote the tangential displacements at the bottom and top surfaces of the first layer. Similarly, in the third layer the displacements of the arbitrary point can be expressed as

$$\mathbf{t}_3(r, \varphi, t) = \frac{1}{2h_3}[(h_3 + r - R_3)u_4(\varphi, t) + (h_3 - r + R_3)u_3(\varphi, t)]\mathbf{e}_\varphi - w(\varphi, t)\mathbf{e}_r,$$

$$R_3 - h_3 \leqslant r \leqslant R_3 + h_3, \tag{2}$$

where $u_3(\varphi,t)$ and $u_4(\varphi,t)$ denote the tangential displacements at the top and bottom surfaces of the third layer. The form of the displacement field over the domain of the second layer is

$$\mathbf{t}_2(r,\varphi,t) = [f(r)u_3(\varphi,t) + g(r)u_2(\varphi,t)]\,\mathbf{e}_\varphi - w(\varphi,t)\mathbf{e}_r, \quad R_2 - h_2 \leqslant r \leqslant R_2 + h_2, \tag{3}$$

where

$$f(R_2 + h_2) = 1, \qquad f(R_2 - h_2) = 0, \tag{4}$$

$$g(R_2 + h_2) = 0, \qquad g(R_2 - h_2) = 1. \tag{5}$$

The functions $f(r)$ and $g(r)$ can be thought of as a shape function through the thickness of the second layer to account for transverse shear effects. The solution of a given problem requires the determination of the unknown functions $u_1(\varphi,t)$, $u_2(\varphi,t)$, $u_3(\varphi,t)$, $u_4(\varphi,t)$, $w(\varphi,t)$, $f(r)$ and $g(r)$. By using

$$\mathbf{t} = u_r\mathbf{e}_r + u_\varphi\mathbf{e}_\varphi, \quad \varepsilon_\varphi = \frac{1}{r}\frac{\partial u_\varphi}{\partial\varphi} + \frac{u_r}{r}, \qquad \gamma_{r\varphi} = \frac{1}{r}\frac{\partial u_r}{\partial\varphi} + \frac{\partial u_r}{\partial r} - \frac{u_\varphi}{r},$$

standard expressions the strain tensor of each layer can be computed from equations (1)–(3)

$$\varepsilon_{\varphi 1} = \frac{1}{r}\left\{\frac{1}{2h_1}\left[(h_1 + r - R_1)\frac{\partial u_2}{\partial\varphi} + (h_1 - r + R_1)\frac{\partial u_1}{\partial\varphi}\right] - w\right\}, \tag{6}$$

$$\gamma_{r\varphi 1} = \frac{1}{r}\left\{-\frac{\partial w}{\partial\varphi} + \frac{1}{2h_1}[(R_1 - h_1)u_2 - (R_1 + h_1)u_1]\right\}, \tag{7}$$

$$\varepsilon_{\varphi 2} = \frac{1}{r}\left[f(r)\frac{\partial u_3}{\partial\varphi} + g(r)\frac{\partial u_2}{\partial\varphi} - w\right], \tag{8}$$

$$\gamma_{r\varphi 2} = -\frac{1}{r}\frac{\partial w}{\partial\varphi} + F(r)u_3 + G(r)u_2, \tag{9}$$

$$\varepsilon_{\varphi 3} = \frac{1}{r}\left\{\frac{1}{2h_3}\left[(h_3 + r - R_3)\frac{\partial u_4}{\partial\varphi} + (h_3 - r + R_3)\frac{\partial u_3}{\partial\varphi}\right] - w\right\}, \tag{10}$$

$$\gamma_{r\varphi 3} = \frac{1}{r}\left\{-\frac{\partial w}{\partial\varphi} + \frac{1}{2h_3}[(R_3 - h_3)u_4 - (R_3 + h_3)u_3]\right\}, \tag{11}$$

where

$$F(r) = \frac{\mathrm{d}f}{\mathrm{d}r} - \frac{f}{r}, \quad \text{and} \quad G(r) = \frac{\mathrm{d}g}{\mathrm{d}r} - \frac{g}{r}.$$

From equation (9), it can be seen that $F(r)$ and $G(r)$ represent the transverse shear strain field through the thickness of the second layer, at a given φ-location. While the assumed form of the shear correction, $f(r)$ and $g(r)$ changes from one iteration to the next, at any given iteration it can be treated as a known function.

The strain energy stored in the circular arch is given by

$$U = \frac{b}{2}\int_{\varphi=0}^{\vartheta}\int_{R_1-h_1}^{R_1+h_1}[E_1(\varepsilon_{\varphi 1})^2 + G_1(\gamma_{r\varphi 1})^2]r\,\mathrm{d}r\,\mathrm{d}\varphi + \frac{b}{2}\int_{\varphi=0}^{\vartheta}\int_{R_2-h_2}^{R_2+h_2}[E_2(\varepsilon_{\varphi 2})^2$$

$$+ G_2(\gamma_{r\varphi 2})^2]r\,\mathrm{d}r\,\mathrm{d}\varphi + \frac{b}{2}\int_{\varphi=0}^{\vartheta}\int_{R_3-h_3}^{R_3+h_3}[E_3(\varepsilon_{\varphi 3})^2 + G_3(\gamma_{r\varphi 3})^2]r\,\mathrm{d}r\,\mathrm{d}\varphi. \tag{12}$$

The kinetic energy, which includes components associated with transverse, in-plane and rotary inertia, is given by

$$T = \frac{b}{2}\int_{\varphi=0}^{\vartheta}\int_{R_1-h_1}^{R_1+h_1}\rho_1(\dot{\mathbf{t}}_1)^2 r\,\mathrm{d}r\,\mathrm{d}\varphi + \frac{b}{2}\int_{\varphi=0}^{\vartheta}\int_{R_2-h_2}^{R_2+h_2}\rho_2(\dot{\mathbf{t}}_2)^2 r\,\mathrm{d}r\,\mathrm{d}\varphi$$

$$+ \frac{b}{2}\int_{\varphi=0}^{\vartheta}\int_{R_3-h_3}^{R_3+h_3}\rho_3(\dot{\mathbf{t}}_3)^2 r\,\mathrm{d}r\,\mathrm{d}\varphi, \tag{13}$$

where the dots over $\mathbf{t}_1$, $\mathbf{t}_2$ and $\mathbf{t}_3$ denote the partial derivative with respect to time. The differential equations of motion and boundary conditions are derived using Hamilton's principle. The equations of motion for the five unknown functions, $u_1(\varphi, t)$, $u_2(\varphi, t)$, $u_3(\varphi, t)$, $u_4(\varphi, t)$ and $w(\varphi, t)$ are

$$A_{11}\frac{\partial^2 u_1}{\partial\varphi^2} + A_{12}\frac{\partial^2 u_2}{\partial\varphi^2} + B_{15}\frac{\partial w}{\partial\varphi} + C_{11}u_1 + C_{12}u_2 = D_{11}\frac{\partial^2 u_1}{\partial t^2} + D_{12}\frac{\partial^2 u_2}{\partial t^2}, \tag{14}$$

$$A_{21}\frac{\partial^2 u_1}{\partial\varphi^2} + A_{22}\frac{\partial^2 u_2}{\partial\varphi^2} + A_{23}\frac{\partial^2 u_3}{\partial\varphi^2} + B_{25}\frac{\partial w}{\partial\varphi} + C_{21}u_1 + C_{22}u_2 + C_{23}u_3$$

$$= D_{21}\frac{\partial^2 u_1}{\partial t^2} + D_{22}\frac{\partial^2 u_2}{\partial t^2} + D_{23}\frac{\partial^2 u_3}{\partial t^2}, \tag{15}$$

$$A_{32}\frac{\partial^2 u_2}{\partial\varphi^2} + A_{33}\frac{\partial^2 u_3}{\partial\varphi^2} + A_{34}\frac{\partial^2 u_4}{\partial\varphi^2} + B_{35}\frac{\partial w}{\partial\varphi} + C_{32}u_2 + C_{33}u_3 + C_{34}u_4$$

$$= D_{32}\frac{\partial^2 u_2}{\partial t^2} + D_{33}\frac{\partial^2 u_3}{\partial t^2} + D_{34}\frac{\partial^2 u_4}{\partial t^2}, \tag{16}$$

$$A_{43}\frac{\partial^2 u_3}{\partial\varphi^2} + A_{44}\frac{\partial^2 u_4}{\partial\varphi^2} + B_{45}\frac{\partial w}{\partial\varphi} + C_{43}u_3 + C_{44}u_4 = D_{43}\frac{\partial^2 u_3}{\partial t^2} + D_{44}\frac{\partial^2 u_4}{\partial t^2}, \tag{17}$$

$$A_{55}\frac{\partial^2 w}{\partial\varphi^2} + B_{51}\frac{\partial u_1}{\partial\varphi} + B_{52}\frac{\partial u_2}{\partial\varphi} + B_{53}\frac{\partial u_3}{\partial\varphi} + B_{54}\frac{\partial u_4}{\partial\varphi} + C_{55}w = D_{55}\frac{\partial^2 w}{\partial t^2}, \tag{18}$$

where A_{ij}, B_{ij}, C_{ij} and D_{ij} are given in Appendix B. K_{1-17} and M_{1-10} are section stiffness and mass coefficients, given by

$$K_{[1,2,3]} = b\int_{R_1-h_1}^{R_1+h_1}\left[r,\,1,\,\frac{1}{r}\right]\mathrm{d}r, \qquad K_{[4,5,6]} = b\int_{R_3-h_3}^{R_3+h_3}\left[r,\,1,\,\frac{1}{r}\right]\mathrm{d}r,$$

$$K_{[7,8,9,10,11,12]} = b\int_{R_2-h_2}^{R_2+h_2}\left[\frac{1}{r}f^2(r),\frac{1}{r}g^2(r),\frac{1}{r}f(r)g(r),\frac{1}{r}f(r),\frac{1}{r}g(r)\right]\mathrm{d}r,$$

$$K_{[13,14,15,16,17]} = b\int_{R_2-h_2}^{R_2+h_2}[rF^2(r),\,rG^2(r),\,F(r),\,G(r),\,rF(r)G(r)]\,\mathrm{d}r,$$

$$M_{[1,2,3]} = b\int_{R_1-h_1}^{R_1+h_1}[r^3,r^2,r]\,\mathrm{d}r, \qquad M_{[4,5,6]} = b\int_{R_2-h_2}^{R_2+h_2}[r^3,r^2,r]\,\mathrm{d}r,$$

$$M_{[7,8,9,10]} = b\int_{R_2-h_2}^{R_2+h_2}[rf^2(r),\;rg^2(r),rf(r)g(r),r]\,\mathrm{d}r. \tag{19}$$

The kinematic and natural boundary conditions specified at $\varphi = 0$ and $\varphi = \vartheta$, are given by

Kinematic		Natural
$u_1 = 0$	or	$F_{11}\dfrac{\partial u_1}{\partial\varphi} + F_{12}\dfrac{\partial u_2}{\partial\varphi} + F_{13}w = 0,$
$u_2 = 0$	or	$F_{21}\dfrac{\partial u_1}{\partial\varphi} + F_{22}\dfrac{\partial u_2}{\partial\varphi} + F_{23}\dfrac{\partial u_3}{\partial\varphi} + F_{24}w = 0,$
$u_3 = 0$	or	$F_{31}\dfrac{\partial u_2}{\partial\varphi} + F_{32}\dfrac{\partial u_3}{\partial\varphi} + F_{33}\dfrac{\partial u_4}{\partial\varphi} + F_{34}w = 0,$
$u_4 = 0$	or	$F_{41}\dfrac{\partial u_3}{\partial\varphi} + F_{42}\dfrac{\partial u_4}{\partial\varphi} + F_{43}w = 0,$
$w = 0$	or	$F_{51}\dfrac{\partial w}{\partial\varphi} + F_{52}u_1 + F_{53}u_2 + F_{54}u_3 + F_{55}u_5 = 0,$

(20)

where F_{ij} are constants. For the special case of a simply supported arch, the first, second, third and fourth natural boundary conditions are combined with the kinematic condition, $w = 0$.

3. SOLUTION FOR A SIMPLY SUPPORTED ARCH

Sinusoidal mode shapes that satisfy the boundary conditions are assumed. Consequently, the assumed displacements are

$$w(\varphi,t) = W\sin(k_n\varphi)\,\mathrm{e}^{\mathrm{i}\omega_n t}, \qquad u_j(\varphi,t) = U_j\cos(k_n\varphi)\mathrm{e}^{\mathrm{i}\omega_n t}, \tag{21}$$

where $k_n = (n\pi)/\vartheta$ and $j = 1$–4. Since the motion is now harmonic, it is legitimate to admit hysteretic damping into the viscoelastic layer by putting complex moduli. The Young's and shear modulus of the constituent materials are represented by the complex quantities

$$E_2^* = E_2(1 + i\alpha_2), \qquad G_2^* = G_2(1 + i\beta_2), \tag{22}$$

where α_2 and β_2 denote the material loss factors in extension and shear respectively. Since the complexes G_2^* and E_2^* are used as complex moduli of the middle layer, the differential equations of motion will have complex coefficients. The substitution of equations (21) into equations (14)–(18), will result in a set of five simultaneous, homogeneous algebraic equations with symmetric and complex coefficients. In matrix form, these equations are

$$[-\omega_n^2[M] + [K]]\{U\} = 0, \qquad \{U\} = \{U_1, U_2, U_3, U_4, W\}, \tag{23}$$

where M_{ij} and K_{ij} given are in Appendix B. The complex eigenvalues give the desired natural frequencies and mode shapes with their phase relations. The natural frequency is approximately equal to the square root of the real part of the eigenvalue. The modal loss factor for the nth mode is approximately equal to the ratio of the imaginary part of the eigenvalue to the real part of the eigenvalue:

$$\eta_n = \mathrm{Im}(\omega_n^2)/\mathrm{Re}(\omega_n^2). \tag{24}$$

4. IMPROVED ESTIMATE FOR SHAPE FUNCTIONS

Improved estimates for the shape functions $f(r)$ and $g(r)$, are derived from the equation of elemental stress equilibrium of the second layer. The equations of motion in plane stress

$$\frac{\partial}{\partial r}[r^2\tau_{r\varphi 2}] + r\frac{\partial \sigma_{\varphi 2}}{\partial \varphi} = r^2\rho_2\frac{\partial^2 u}{\partial t^2}, \tag{25}$$

$$\frac{\partial \tau_{r\varphi 2}}{\partial \varphi} - \sigma_{\varphi 2} = r\rho_2\frac{\partial^2 w}{\partial t^2}, \tag{26}$$

applied to the second layer of the arch with $\sigma_{\varphi 2} = E_2\varepsilon_{\varphi 2}$, $\tau_{r\varphi 2} = G_2\gamma_{r\varphi 2}$ expressions, are now in the form

$$G_2\frac{\partial}{\partial r}\left\{-r\frac{\partial w}{\partial \varphi} + r^2\left[\frac{\mathrm{d}f}{\mathrm{d}r} - \frac{f}{r}\right]u_3 + r^2\left[\frac{\mathrm{d}g}{\mathrm{d}r} - \frac{g}{r}\right]u_2\right\}$$

$$+ E_2\left[f(r)\frac{\partial^2 u_3}{\partial \varphi^2} + g(r)\frac{\partial^2 u_2}{\partial \varphi^2} - \frac{\partial w}{\partial \varphi}\right] = r^2\rho_2\left[f(r)\frac{\partial^2 u_3}{\partial t^2} + g(r)\frac{\partial^2 u_2}{\partial t^2}\right], \tag{27}$$

$$G_2\left[-\frac{1}{r}\frac{\partial^2 w}{\partial \varphi^2} + \left(\frac{\mathrm{d}f}{\mathrm{d}r} - \frac{f}{r}\right)\frac{\partial u_3}{\partial \varphi} + \left(\frac{\mathrm{d}g}{\mathrm{d}r} - \frac{g}{r}\right)\frac{\partial u_2}{\partial \varphi}\right]$$

$$- \frac{E_2}{r}\left[f(r)\frac{\partial u_3}{\partial \varphi^2} + g(r)\frac{\partial u_2}{\partial \varphi^2} - w\right] = r\rho_2\frac{\partial^2 w}{\partial t^2}. \tag{28}$$

From equations (21), it is obvious that

$$\frac{\partial^2 w}{\partial \varphi^2} = -k_n^2 w, \qquad \frac{\partial^2 w}{\partial t^2} = -\omega_n^2 w, \tag{29}$$

$$\frac{\partial^2 u_2}{\partial \varphi^2} = -k_n^2 u_2, \qquad \frac{\partial^2 u_2}{\partial t^2} = -\omega_n^2 u_2, \tag{30}$$

$$\frac{\partial^2 u_3}{\partial \varphi^2} = -k_n^2 u_3, \qquad \frac{\partial^2 u_3}{\partial t^2} = -\omega_n^2 u_3. \tag{31}$$

If equations (29) are substituted into equation (28) it is found that

$$w(\varphi, t) = \frac{1}{G_2 k_n^2 + E_2 + r^2 \rho_2 \omega_n^2} \left\{ \left[-G_2 r \frac{\mathrm{d}f}{\mathrm{d}r} + (G_2 + E_2) f \right] \frac{\partial u_3}{\partial \varphi} + \left[-G_2 r \frac{\mathrm{d}g}{\mathrm{d}r} + (G_2 + E_2) g \right] \frac{\partial u_2}{\partial \varphi} \right\}. \tag{32}$$

Substitution of the function $w(\varphi, t)$ into equation (27) with relations (30) and (31), gives

$$\left[r^2 \frac{\mathrm{d}^2 f}{\mathrm{d}r^2} + r(1 - P(r)) \frac{\mathrm{d}f}{\mathrm{d}r} + Q(r) f(r) \right] u_3(\varphi, t) + \left[r^2 \frac{\mathrm{d}^2 g}{\mathrm{d}r^2} + r(1 - P(r)) \frac{\mathrm{d}g}{\mathrm{d}r} + Q(r) g(r) \right] u_2(\varphi, t) = 0, \tag{33}$$

where

$$P(r) = \frac{(E_2 + G_2) k_n^2}{(G_2 k_n^2 + E_2 + r^2 \rho_2 \omega_n^2)}, \tag{34}$$

$$Q(r) = -1 - \frac{(E_2 k_n^2 - r^2 \rho_2 \omega_n^2)}{G_2} + \frac{(E_2 + G_2)^2 k_n^2}{G_2 (G_2 k_n^2 + E_2 + r^2 \rho_2 \omega_n^2)}. \tag{35}$$

Using the boundary conditions (4) and (5) for $f(r)$ and $g(r)$, respectively, from equation (33) the following two boundary value problems are obtained:

$$r^2 \frac{\mathrm{d}^2 f}{\mathrm{d}r} + r(1 - P(r)) \frac{\mathrm{d}f}{\mathrm{d}r} + Q(r) f(r) = 0,$$

$$f(R_2 - h_2) = 0, \qquad f(R_2 + h_2) = 1 \tag{36}$$

and

$$r^2 \frac{\mathrm{d}^2 g}{\mathrm{d}r^2} + r(1 - P(r)) \frac{\mathrm{d}g}{\mathrm{d}r} + Q(r) g(r) = 0,$$

$$g(R_2 - h_2) = 1, \qquad g(R_2 + h_2) = 0. \tag{37}$$

TABLE 1

Comparison of fundamental frequency and loss factor with results from reference [13] *for a flat sandwich beam*

	[13]		Present theory			
	$\alpha_2 = 0{\cdot}1$		$\alpha_2 = 0{\cdot}1$		$\alpha_2 = 0$	
ϑ(rad)	f(Hz)	η	f(Hz)	η	f(Hz)	η
0·016	$5{\cdot}99 \times 10^4$	0·0322	$6{\cdot}005 \times 10^4$	0·0317	$6{\cdot}01 \times 10^4$	0·0295
0·026	$3{\cdot}04 \times 10^4$	0·0403	$3{\cdot}04 \times 10^4$	0·0398	$3{\cdot}04 \times 10^4$	0·0377
0·036	$1{\cdot}896 \times 10^4$	0·04	$1{\cdot}9 \times 10^4$	0·0395	$1{\cdot}894 \times 10^4$	0·0377
0·046	$1{\cdot}3 \times 10^4$	0·036	$1{\cdot}309 \times 10^4$	0·0359	$1{\cdot}304 \times 10^4$	0·0341
0·056	$9{\cdot}57 \times 10^3$	0·0319	$9{\cdot}57 \times 10^3$	0·0314	$9{\cdot}54 \times 10^3$	0·0296
0·066	$7{\cdot}295 \times 10^3$	0·0276	$7{\cdot}296 \times 10^3$	0·0273	$7{\cdot}27 \times 10^3$	0·0253
0·076	$5{\cdot}734 \times 10^3$	0·024	$5{\cdot}734 \times 10^3$	0·0236	$5{\cdot}718 \times 10^3$	0·0215
0·086	$4{\cdot}618 \times 10^3$	0·02099	$4{\cdot}616 \times 10^3$	0·0206	$4{\cdot}606 \times 10^3$	0·0184
0·096	$3{\cdot}79 \times 10^3$	0·0184	$3{\cdot}79 \times 10^3$	0·0181	$3{\cdot}785 \times 10^3$	0·0158
0·16	$1{\cdot}46 \times 10^3$	0·0099	$1{\cdot}458 \times 10^3$	0·00976	$1{\cdot}467 \times 10^3$	0·00697

The functions $f(r)$ and $g(r)$ are influenced by both elastic and inertial effects, the relative importance of each depending on the mode. The elastic component typically predominates, except at a very high frequency. In general, the solution of problems (36) and (37) has no closed-form solution. In the present implementation, the solution is performed numerically using the finite difference method.

5. RESULTS AND DISCUSSION

In this section numerical results are presented. The damped natural frequency and loss factor of a sandwich circular arch with the following specifications are computed: $E_1 = E_3 = 2{\cdot}068 \times 10^{11}$ Pa; $\rho_1 = \rho_3 = 7850\,\text{kg/mm}^3$; $G_2 = 9{\cdot}8 \times 10^9$ Pa; $E_2 = 3G_2$; $\beta_2 = 0{\cdot}1$; $h_1 = 4\,\text{mm}$; $h_2 = 2{\cdot}5\,\text{mm}$; $h_3 = 1{\cdot}5\,\text{mm}$; $\rho_2 = 2600\,\text{kg/mm}^3$; $R_1 = 993{\cdot}5\,\text{mm}$; $R_2 = 1000\,\text{mm}$; $R_3 = 1004\,\text{mm}$.

The structure considered is variable length of the arch ($L = 16$–160 mm). The loss factor was compared with the values obtained by Zapfe and Lesieutre in reference [22] for a flat sandwich beam. For a given developed length, if the sandwich ring segment with a very large radius is assumed to have a very small opening angle, it becomes geometrically close to a flat beam. The loss factors thus obtained showed excellent agreement with Zapfe and Lesieutre' results in reference [22]. This agreement is despite the different model in facesheet.

Most of the earlier theories have ignored the material loss factor in the extension in the core to obtain simpler theories, $\alpha_2 = 0$. However this restriction may not be valid for a short, thick cored circular arch. Table 1 thus compares the effect of ignoring α_2 on the loss factor as a function of the angle of the arch. This table shows that the effect of ignoring α_2 is the reduction in the bending mode loss factor.

The eigenproblem of the plane bending of circular arch shaped layered beams was investigated by using the finite element method [23]. The comparison between different approaches makes it possible to obtain more accurate and realistic results. The test example to be investigated is a three-layered circular ring segment containing two elastic layers of

TABLE 2

Comparison of natural frequencies using different methods (Hz)

n	[13, 24]	[23] Solid elements	Present theory	[23] Shell elements
1	18·72	18·17	17·2	15·55
2	94·83	95·50	88·91	84·68
3	210·41	216·40	202·2	197·53
4	353·10	371·52	340·09	348·15

3 mm thickness and a core of 8 mm thickness. This structure is investigated for constant radius $R_2 = 140$ mm and constant, ($\vartheta = \pi/2$) angle of arch. The width of the ring is 6 mm. The material properties of the circular arch are the following: $E_1 = E_3 = 2{\cdot}1 \times 10^2\ \mathrm{N/mm^2}$; $E_2 = 0{\cdot}6 \times 10^2\ \mathrm{N/mm^2}$; $G_1 = E_1/2{\cdot}5$; $G_2 = E_2/2{\cdot}5$; $G_3 = G_1$; $\rho_1 = 7{\cdot}8 \times 10^{-6}\ \mathrm{kg/mm^3}$; $\rho_2 = 2{\cdot}7 \times 10^{-6}\ \mathrm{kg/mm^3}$; $\rho_3 = \rho_1$.

The finite element model of the structure has two–two elements along the face thickness and three elements along the thickness of the core. The two edges of the circular arch are simply supported. This model consists of eight node hexahedron 3-D elements (280 pcs.). An other possible way of building the model of this structure is by using four node composite shell elements. The model contains the number of elements along the length. As a composite shell element contains the properties of the layers, this model contains only 40 elements, so the calculation time is much less than in the case of hexahedron elements. The analytical results are compared with the results of the two different finite element models in Table 2.

A flexure of the three-layer sandwich arch results in energy dissipation due to strains induced in the viscoelastic layer. In a symmetrical arrangement with identical elastic layers, most of the damping is due to the shear of viscoelastic layer. In an unsymmetrical arrangement, with dissimilar elastic layers, one might expect damping due to a direct strain as well as shear in the viscoelastic layer, the former being known as extensional damping and the latter as shear damping. Both these effects have been included by Kovacs [13, 24]. However, the stress–strain law assumed for the viscoelastic layer was not strictly correct and was only an approximation if extensional effects were considered. A comparison between the present complete approach and that of reference [13] is given in Table 3 for a specific case with the following values: $E_1 = E_3 = 0{\cdot}736 \times 10^5\ \mathrm{N/mm^2}$; $G_1 = G_3 = E_3/2{\cdot}5$; $h_2 = 0{\cdot}1$ mm; $n = 1$; $\rho_1 = \rho_3 = 0{\cdot}28 \times 10^{-8}\ \mathrm{Ns/mm^4}$; $\rho_2 = \rho_3/2$; $\beta_2 = \alpha_2 = 1{\cdot}0$; $h_3 = 3$ mm; $E_2 = 0{\cdot}133 \times 10^3\ \mathrm{N/mm^2}$; $G_2 = E_2/3$; $R_2 = 1000$ mm; $h_1 = 16{\cdot}9$ mm.

A significant difference is seen for the long circular arch and a smaller value of the modal number $n = 1$. For a central angle of the circular arch $\vartheta = 1, 2$ (rad), the loss factor obtained by using the equations of Kovacs [13] is negative which is physically impossible. The comparison of the damping effectiveness obtained by the two approaches gives significant differences for a long circular arch having a constrained viscoelastic layer with a high value of shear modulus. The difference is most marked for the lower resonant modes (low values of the modal number n). Errors in excess of 100 percent have been calculated, with the previous work providing an underestimation of the damping effectiveness. The higher the value of the shear modulus, the more important the contribution from the extensional stress becomes. This in turn affects the shear stress distribution, which is no longer constant across the damping layer as it has been assumed in the previous work.

TABLE 3

Comparison of fundamental frequency and loss factor with results from reference [13] *for a circular ring segment*

	[13]		Present theory	
ϑ(rad)	f(Hz)	η	f(Hz)	η
0·1	$7{\cdot}75 \times 10^3$	0·003	$7{\cdot}89 \times 10^3$	0·00286
0·2	$2{\cdot}19 \times 10^3$	0·0023	$2{\cdot}24 \times 10^3$	0·0021
0·3	$9{\cdot}96 \times 10^2$	0·002	$1{\cdot}01 \times 10^3$	0·002
0·4	$5{\cdot}61 \times 10^2$	0·0021	$5{\cdot}73 \times 10^2$	0·00194
0·5	$3{\cdot}56 \times 10^2$	0·0013	$3{\cdot}63 \times 10^2$	0·00192
0·6	$2{\cdot}44 \times 10^2$	0·0011	$2{\cdot}49 \times 10^2$	0·00191
0·7	$1{\cdot}76 \times 10^2$	0·002	$1{\cdot}79 \times 10^2$	0·0019
0·8	$1{\cdot}32 \times 10^2$	0·0029	$1{\cdot}34 \times 10^2$	0·00189
0·9	$1{\cdot}02 \times 10^2$	0·00048	$1{\cdot}03 \times 10^2$	0·00183
1·0	$7{\cdot}9 \times 10$	0·00012	$8{\cdot}14 \times 10$	0·00179
1·1	$6{\cdot}23 \times 10$	0·0143	$6{\cdot}51 \times 10$	0·00187
1·2	$4{\cdot}72 \times 10$	− 0·001	$5{\cdot}27 \times 10$	0·00187

6. CONCLUSIONS

A new iterative laminate model has been presented for a sandwich circular arch that can determine accurately the loss factor in short as well as long, stiff cored sandwich arches. This represents an advance over the previous laminate models, in which accurate estimates of the loss factor were only possible if short, stiff cored sandwich arches were investigated.

REFERENCES

1. P. CHIDAMPARAM and A. W. LEISSA 1993 *Applied Mechnics Review* **46**, 467–483. Vibrations of planar curved beams, rings, and arches.
2. P. A. A. LAURA and M. J. MAURIZI 1987 *The Shock and Vibration Digest* **19**, 6–9. Recent research on vibrations of arch-type structures.
3. S. MARKUS and T. NANASI 1981 *The Shock and Vibration Digest* **7**, 3–14. Vibrations of curved beams.
4. R. DAVIS, R. D. HENSHELL and G. B. WARBURTON 1972 *Journal Sound and Vibration* **25**, 561–576. Constant curvature beam finite elements for in-plane vibration.
5. K. M. AHMED 1971 *Journal Sound and Vibration* **18**, 61–74. Free vibrations of curved sandwich beams by the method of finite elements.
6. K.M.AHMED 1972 *Journal Sound and Vibration* **21**, 263–276. Dynamic analysis of sandwich beams.
7. R. A. DI. TARANTO 1973 *Journal of the Acoustical Society of America* **53**, 748–757. Free and forced response of a laminated ring.
8. Y. P. LU and B. E. DOUGLAS 1974 *Journal Sound and Vibration* **32**, 513–516. On the forced vibrations of three-layer damped sandwich ring.
9. M. J. SAGARTZ 1977 *Journal Applied Mechanics* **44**, 299–304. Transient response of three-layered rings.
10. A. TATEMICHI, A. OKAZAKI and M. HIKAYAMA 1980 *Bulletin Nagaya Institute* **29**, 309–317. Damping properties of curved sandwich beams with viscoelastic layer.
11. F. C. NELSON and D. F. SULLIVAN 1977 *Journal of American Society of Mechanical Engineers* **154**, 1–8. The forced vibrations of a three-layer damped arcular ring.
12. O. K. ISVAN and F. C. NELSON 1982 *Mecanique Materiaux Electricite* 394–395, 447–449. Free vibrations of a three-layer damped circular ring segment.

13. B. KOVACS 1996 *Publications of the University of Miskolc* **36**, 65–76. Free vibrations of a layered damped arch.
14. C. LIAO and J. N. REDDY 1990 *Computers and Structures* **34**, 805–815. Analysis of aniso-tropic, striffened compusite laminates using a continuum-based shell element.
15. A. BHIMARADDI, A. J. CARR and P. J. MOSS 1989 *Computers and Structures* **31**, 309–317. Generalized finite element analysis of laminated curved beams with constant curvature.
16. M. S. QATU 1992 *Journal of Sound and Vibration* **159**, 327–338. In-plane vibration of slightly curved laminated composite beams.
17. M. S. QATU and A. A. ELSHARKAWY 1993 *Computers and Structures* **47**, 305–311. Vibration of laminated composite arches with deep curvature and arbitrary boundaries.
18. M. S. QATU 1992 *International Journal of Solid and Structures* **30**, 2743–2756. Equations for the analysis of thin and moderately thick laminated composite curved beams.
19. V. YILDIRIM 1999 *Journal of Sound and Vibration* **224**, 575–589. Rotary inertia, axial and shear deformation effects on the in-plane natural frequencies of symmetric cross-ply laminated circular arches.
20. J. VASWANI, N. T. ASNANI and B. C. NAKRA 1988 *Composite structures* **10**, 231–245. Vibration and damping analysis of curved sandwich beams with a viscoelastic core.
21. S. HE and M. D. RAO 1992 *Journal of Sound and Vibration* **159**, 101–113. Prediction of loss factors of curved sandwich beams.
22. J. A. ZAPFE and G. A. LESIEUTRE 1997 *Journal of Sound and Vibration* **199**, 275–284. Vibration analysis of laminated beams using an iterative smeared laminate model.
23. B. KOVACS, F. J. SZABO and A. DOBROCZONI 1993 *microCAD-SYSTEM* '93 *International Computer Science Meeting Proceeding*, *Miskolc*, *Hungary*, 65–77. Free vibrations of a layered circular ring segment .
24. B. KOVACS 1992 *Ph.D. thesis*, *University of Miskolc*, *Miskolc*, *Hungary*. Vibration and stability of layered circular arch.

APPENDIX A

Equations (14)–(18) in the main text contain certain A_{ij}, B_{ij}, C_{ij} and D_{ij} terms which are defined as follows:

$$A_{11} = -E_1K_1\left(\frac{1}{2h_1}\right)^2 + 2E_1K_2\left(\frac{1}{2h_1}\right)^2(h_1 + R_1) - E_1K_3\left(\frac{h_1 + R_1}{2h_1}\right)^2,$$

$$A_{12} = E_1K_1\left(\frac{1}{2h_1}\right)^2 + E_1K_2\left(\frac{1}{2h_1}\right)^2(h_1 - R_1) - E_1K_2\left(\frac{1}{2h_1}\right)^2(h_1 + R_1)$$

$$- E_1K_3\left(\frac{1}{2h_1}\right)^2(h_1 - R_1)(h_1 + R_1),$$

$$B_{15} = G_1K_3\left(\frac{R_1 + h_1}{2h_1}\right) - E_1K_2\left(\frac{1}{2h_1}\right) + E_1K_3\left(\frac{1}{2h_1}\right)(h_1 + R_1),$$

$$C_{11} = G_1K_3\left(\frac{R_1 + h_1}{2h_1}\right)^2,$$

$$C_{12} = -G_1K_3\left(\frac{1}{2h_1}\right)^2(R_1 - h_1)(R_1 + h_1),$$

$$D_{11} = -\rho_1M_1\left(\frac{1}{2h_1}\right)^2 + 2\rho_1M_2\left(\frac{1}{2h_1}\right)^2(h_1 + R_1) - \rho_1M_3\left(\frac{h_1 + R_1}{2h_1}\right)^2,$$

$$D_{12} = \rho_1 M_1 \left(\frac{1}{2h_1}\right)^2 + \rho_1 M_2 \left(\frac{1}{2h_1}\right)^2 (h_1 - R_1) - \rho_1 M_2 \left(\frac{1}{2h_1}\right)^2 (h_1 + R_1)$$

$$- \rho_1 M_3 \left(\frac{1}{2h_1}\right)^2 (h_1 + R_1)(h_1 - R_1),$$

$$A_{22} = - E_1 K_1 \left(\frac{1}{2h_1}\right)^2 - E_1 K_2 \left(\frac{1}{2h_1}\right)^2 (h_1 - R_1) - E_1 K_2 \left(\frac{1}{2h_1}\right)^2 (h_1 - R_1)$$

$$- E_1 K_3 \left(\frac{h_1 - R_1}{2h_1}\right)^2 - E_2 K_8,$$

$$A_{23} = - E_2 K_{10},$$

$$B_{25} = - G_1 K_3 \frac{R_1 - h_1}{2h_1} - G_2 K_{16} + E_1 K_2 \frac{1}{2h_1} + E_1 K_3 \left(\frac{h_1 - R_1}{2h_1}\right) + E_2 K_{12},$$

$$C_{22} = G_1 K_3 \left(\frac{R_1 - h_1}{2h_1}\right)^2 + G_2 K_{14},$$

$$C_{23} = G_2 K_{17},$$

$$D_{22} = - \rho_1 M_1 \left(\frac{1}{2h_1}\right)^2 - 2\rho_1 M_2 \left(\frac{1}{2h_1}\right)^2 (h_1 - R_1) - \rho_1 M_3 \left(\frac{1}{2h_1}\right)^2 (h_1 - R_1)^2 + \rho_2 M_8,$$

$$D_{23} = - \rho_2 M_9,$$

$$A_{33} = - E_3 K_4 \left(\frac{1}{2h_3}\right)^2 + E_3 K_5 \left(\frac{1}{2h_3}\right)^2 (h_3 + R_3) + E_3 K_5 \left(\frac{1}{2h_3}\right)^2 (h_3 + R_3)$$

$$- E_3 K_6 \left(\frac{h_3 + R_3}{2h_3}\right)^2 - E_2 K_7,$$

$$A_{34} = E_3 K_4 \left(\frac{1}{2h_3}\right)^2 + E_3 K_5 \left(\frac{1}{2h_3}\right)^2 (h_3 - R_3) - E_3 K_5 \left(\frac{1}{2h_3}\right)^2 (h_3 + R_3)$$

$$- E_3 K_6 \left(\frac{1}{2h_3}\right)^2 (h_3 - R_3)(h_3 + R_3),$$

$$B_{35} = G_3 K_6 \left(\frac{R_3 + h_3}{2h_3}\right) - G_2 K_{15} - E_3 K_5 \left(\frac{1}{2h_3}\right) + E_3 K_6 \left(\frac{h_3 + R_3}{2h_3}\right) + E_2 K_{11},$$

$$C_{33} = G_3 K_6 \left(\frac{R_3 + h_3}{2h_3}\right)^2 + G_2 K_{13},$$

$$C_{34} = -G_3K_6\left(\frac{1}{2h_3}\right)^2(R_3 - h_3)(R_3 + h_3),$$

$$D_{33} = -\rho_3M_4\left(\frac{1}{2h_3}\right)^2 + 2\rho_3M_5\left(\frac{1}{2h_3}\right)^2(h_3 + R_3) - \rho_3M_6\left(\frac{h_3 + R_3}{2h_3}\right)^2 - \rho_2M_7,$$

$$D_{34} = \rho_3M_4\left(\frac{1}{2h_3}\right)^2 + 2\rho_3M_5\left(\frac{1}{2h_3}\right)^2(h_3 - R_3) - \rho_3M_5\left(\frac{1}{2h_3}\right)^2(h_3 + R_3)$$
$$- \rho_3M_6\left(\frac{1}{2h_3}\right)^2(h_3 + R_3)(h_3 - R_3),$$

$$A_{44} = -E_3K_4\left(\frac{1}{2h_3}\right)^2 - E_3K_5\left(\frac{1}{2h_3}\right)^2(h_3 - R_3) - E_3K_6\left(\frac{h_3 - R_3}{2h_3}\right)^2,$$

$$B_{45} = -G_3K_6\left(\frac{R_3 - h_3}{2h_3}\right)^2 + E_3K_5\frac{1}{2h_3} + E_3K_6\left(\frac{h_3 - R_3}{2h_3}\right),$$

$$C_{44} = G_3K_6\left(\frac{R_3 - h_3}{2h_3}\right)^2,$$

$$D_{44} = -\rho_3M_4\left(\frac{1}{2h_3}\right)^2 - 2\rho_3M_5\left(\frac{1}{2h_3}\right)^2(h_3 - R_3) - \rho_3M_6\left(\frac{h_3 - R_3}{2h_3}\right)^2,$$

$$A_{55} = -G_1K_3 - G_3K_6 - G_2K_9,$$

$$C_{55} = E_1K_3 + E_3K_6 + E_2K_9,$$

$$D_{55} = -\rho_1M_3 - \rho_3M_6 - \rho_2M_{10},$$

$$A_{ij} = A_{ji}, \qquad B_{ij} = -B_{ji}, \qquad C_{ij} = C_{ji}, \qquad D_{ij} = D_{ji}, \qquad i,j = 1,2,\ldots,5.$$

Equation (23) in the main text contain K_{ij} and M_{ij} terms which are defined as follows:

$$K_{ij} = -k_n^2A_{ij} + k_n|B_{ij}| + C_{ij}, \qquad M_{ij} = -D_{ij}, \qquad i,j = 1,2,\ldots,5.$$

APPENDIX B: NOMENCLATURE

b	width of the arch
E_i	elastic modulus of layer i
E_2^*	complex modulus in tension
$\mathbf{e}_r$	unit vector in the radial direction
$\mathbf{e}_\varphi$	unit vector in the transverse direction
$\mathbf{e}_z$	unit vector in the z direction
$\varepsilon_{\varphi i}$	tensile strain of layer i
$f(r)$	shape function
$g(r)$	shape function
G_i	shear modulus of layer i
G_2^*	complex modulus in shear
$\gamma_{r\varphi i}$	shear strain of layer i
h_i	half-thickness of layer i
φ	circumferential co-ordinate
n	mode number

r	cylindrical co-ordinate
R_i	radius of center line of layer i
T	kinetic energy
$\sigma_{\varphi i}$	tensile stress of layer i
$\tau_{r\varphi i}$	shear stress of layer i
$\mathbf{t}_i$	displacement vector of layer i
u_1	tangential displacement at the bottom of the first layer
u_2	tangential displacement at the top of the first layer
u_3	tangential displacement at the bottom of the third layer
u_4	tangential displacement at the top of the third layer
α_2	material loss factor in tension of the second layer
β_2	material loss factor in shear of the second layer
η_n	composite loss factor for the nth mode
ω_n	frequency of oscillation in radians for the nth mode
f_n	frequency of oscillation in Hertz for the nth mode
ρ_i	density of layer i
ϑ	opening angle of ring segment
w	radial-displacement component